Bioprocess Biosyst Eng (2015) 38:711–719
DOI 10.1007/s00449-014-1311-5

ORIGINAL PAPER

Synthesis, characterization and kinetics of formation of silver nanoparticles by reduction with adrenaline in the micellar media

M. Z. A. Rafiquee · Masoom R. Siddiqui · Mohd Sajid Ali · Hamad A. Al-Lohedan · Z. A. Al-Othman

Received: 25 February 2014 / Accepted: 15 October 2014 / Published online: 26 October 2014

Abstract The present paper describes about the easy, simple and convenient procedure for the synthesis of silver nanoparticles (Ag-NPs) in aqueous solutions by the reduction of silver nitrate with adrenaline. The surfactant molecules of cetyltrimethylammonium bromide (CTABr) and sodium dodecyl ate (SDS) behaved differently during the reduction of Ag^+ ions by adrenaline. The obtained data suggest that the variation of [CTABr] gave a maxima-like curve for rate constant versus [CTABr], while, the values of rate constant decreased with the increase in [SDS]. The addition of surfactant molecules stabilized the Ag-NPs. The UV–Visible spectra were analyzed to deduce the particle size. The calculated sizes of the nanoparticles were further compared by the TEM images. The XRD spectrum confirmed the crystalline nature of silver nanoparticles having the face-centered cubic crystal structure. The edge length of unit cell was found 4.076 Å. The kinetics of formation of Ag-NPs was performed at different concentrations of adrenaline, $AgNO_3$, NaOH and [surfactant]. The values of rate constant were independent on [adrenaline] and [$AgNO_3$]. The increase in [NaOH] increased the rate of agglomeration of silver particles to form Ag-NPs. A linear relationship was obtained for the plot of rate constant versus [NaOH].

Keywords Silver nanoparticle · Adrenaline · Kinetics · CTABr · SDS · TEM

Introduction

The nano sized metal particles have exhibited distinct physical, biological and chemical properties as compared to their bulk counterparts. These special properties are due to small particle dimensions and high surface areas. Size and shape-dependent properties of the nanoparticles makes them applicable in wide range of interest i.e., catalyst, sensing, data storage and antibacterial activity. One of the most important applications of the silver nanoparticle is its role as antibacterial agents in food storage, health industries and textile coating in addition to the environmental usage. The studies on metal nanoparticles gained tremendous significance because of its potential technological applications in almost all the important fields including electronics, photography, catalysis, biological labeling, photonics, optoelectronics, surface-enhanced Raman scattering (SERS) detection etc. [1–6]. The metal nanoparticles can be synthesized through two approaches; first being the physical one involving laser ablation and evaporation or condensation. The laser ablation method has a peculiar advantage of having absence of any chemical reagents, thus, resulting into the production of pure colloids for further application. The other being the chemical approach in which the reduction of meal ions results in the formation of minute metal clusters [7–10]. One of the important advantages associated with the synthesis of the nanoparticles in solution is the ease with which the design, shape and

Electronic supplementary material The online version of this article (doi:10.1007/s00449-014-1311-5) contains supplementary material, which is available to authorized users.

M. Z. A. Rafiquee (✉) · M. S. Ali · H. A. Al-Lohedan
Surfactant Research Chair, Department of Chemistry, College of Science, King Saud University, Riyadh 11541, Saudi Arabia
e-mail: drrafiquee@gmail.com

M. R. Siddiqui · Z. A. Al-Othman
Advanced Materials Research Chair, Department of Chemistry, College of Science, King Saud University, Riyadh 11541, Saudi Arabia

size of the nanoparticles can be precisely controlled. The synthesis of metal nanoparticles needs metal precursor, reducing agent and stabilizing agent. The reducing agents first reduce silver ions (Ag^{+}) into metallic silver (Ag^{0}) and, thereafter, the metallic silver undergoes nucleation and agglomeration into oligomeric clusters (growth stages). Besides controlling the shape and size of the nanoparticles, the stabilizer prevents further agglomeration and sedimentation of the colloidal nanoparticles [11–13].

Silver nanoparticles are believed to be nontoxic for human health as its products are approved by US FDA, US EPA and various other accreditation agencies [7]. The shape, size and the non-toxicity of the silver nanoparticle makes them high in demand in disinfecting the home appliances, medical devices and in water treatment. Among the most recent applications of the silver nanoparticles include the wound dressing by incorporating silver nanoparticles. The in vitro results are shown to have an efficacy of >99.99 % for *Staphylococcus aureus* and able to kill entire *Pseudomonas aeruginosa* cultures [14]. Silver nanoparticles coated surgical masks were reported to be capable of reduction in viable *S. aureus* and *E. coli* cells after incubation [15]. In yet another latest biological application of nanoparticles, gold nanoparticle entrapped within the polyaniline layer was developed for amperometric glucose sensor [16]. The Au-NPs included in GOx/Au-NPs/PANI nanocomposites significantly increased the amperometric signal. In a similar study, Ramanaviciene et al. [17] evaluated the efficiency of gold nanoparticles (Au-NP) for enzymatic activity of glucose oxidase. The gold nanoparticles together with *N*-methylphenazonium methyl sulfate have increased the rate of glucose oxidase catalyzed enzymatic reaction. Their results show that the gold nanoparticles effectively transfer electrons from glucose oxidase to red-ox-dye 2,6-dichloroindophenol sodium salt hydrate and at some conditions electron transfer via gold nanoparticles is comparable with electron transfer via red-ox mediator *N*-methylphenazonium methyl sufate. Oztekin et al. [18] reported the use of copper nanoparticle modified carbon electrode for the determination of dopamine. They demonstrated that glassy carbon electrode modified by copper nanoparticles is suitable for the determination of dopamine in real samples such as human blood serum.

One of the advantages associated with the synthesis of the metal nanoparticles in solution phase is its manipulation into the desirable shape and size. It can be readily achieved through adjusting the reaction parameters such as concentration, temperature, pH, reducing ability, etc. The reducing ability of the reductant and stabilizing agents play crucial role in determining the shape and size of the obtained nanoparticles [19, 20]. For, example, the size of Ag-NPs obtained by Velikov et al. [21] was up to 1,200 nm on reduction of silver nitrate by ascorbic acid while the reduction by polyols at high refluxing temperatures gave rise to Ag-NPs of ~40 nm size [22, 23]. Raveendran et al. [24] reported the synthesis of Ag-NPs of small size Ag-NPs (~5 nm) by using β-D-glucose as reducing agent and starch as the stabilizing agent. Similarly, Ag-NPs of ~20 nm were reportedly obtained by using heparin as a reducing/capping agent and the silver nanocubes (with edge length of 55 ± 5 nm) were obtained on reduction of $[Ag(NH_3)_2]^{+}$ with glucose in the presence of *n*-hexadecyltrimethylammonium bromide (HTABr) [25, 26]. Hussain et al. [27–29] reported the synthesis of the silver nanoparticles through the plant extracts, a viable green chemical route to the preparation of stable bio-conjugated silver nanostructures.

In the following paper, attempts were made to synthesize and study the rate of formation of Ag-NPs through the reduction of silver nitrate by adrenaline. Adrenaline (Epinephrine) is among the catecholamines used to regulate myocardial contractility and metabolism; and play a prominent role in cardiac physiology [30–32]. It contains oxidizable catechol and basic amine, and has tendency to undergo autoxidation in alkaline medium [33]. Thus, adrenaline is among the soft reducing agent and the studies will help to understand the fate of Ag^{+} ions in the presence of adrenaline in the biological fluids. Based on the kinetic studies, the mechanism of the reaction is proposed in this paper.

Experimental

Materials

1-(3,4-Dihydroxyphenyl)-2-methylamino ethanol (Adrenaline, 95 %, Aldrich, USA), silver nitrate (99 %), cetyltrimethylammonium bromide (CTABr, 99 %, Aldrich), sodium dodecyl sulfate (SDS, 99 %, BDH, England) sodium hydroxide of Anal R grade were used during the experiments. The stock solutions of $AgNO_3$; 1.0×10^{-2} mol dm^{-3}, adrenaline; 1.0×10^{-2} mol dm^{-3}, surfactant; 1.0×10^{-1} mol dm^{-3} and NaOH; 1.0×10^{-2} mol dm^{-3} were prepared in the deionized double-distilled water having the specific conductance: $1-2 \times 10^{-6}$ Ω^{-1} cm^{-1}. The reagents were further diluted when needed, and the appropriate amounts of these chemicals were used during the kinetic experiments.

Instruments

The spectral studies were carried out by using Perkin-Elmer Lambda 650 UV–visible spectrophotometer attached with quartz cuvette having 1 cm path length. The

temperature was kept constant at 25.0 ± 0.1 °C with L.K.B. 2,209 multi-temperature water bath. The transmission electron microscopy (TEM) was performed with JEOL ultra-high resolution field emission electron microscope (model JEM 2100F) with an accelerating voltage of 200 kV. The XRD patterns were recorded by X-ray diffractometer (Rigaku, Ultima IV, Germany) equipped with CuKα ($\lambda = 1.54056$ Å) radiation source operated in the $\theta/2\theta$ mode in the 10°–80° (2θ) range with the step-scan of $2\theta = 0.01°$.

Kinetic measurements

The preliminary experiments have demonstrated that the addition of silver nitrate solution to the alkaline adrenaline solution gave deep orange colored product (Supplementary material, S1 (a)). The characterization of the orange colored product by spectral and TEM studies confirmed the formation of silver nanoparticles. The maximum value of absorbance (λ_{max}) was observed at 426 nm wavelengths. The spectra were recorded under the different experimental conditions by varying the concentrations of $AgNO_3$, adrenaline, surfactant and NaOH to establish the role of each reagent in the color yield and on the rate of formation of silver nanoparticles. The required amounts of the reactants ($AgNO_3$, adrenaline, surfactant and NaOH) were taken into the 3 mL cuvette. The kinetics experiments for the rate of formation of silver nanoparticles in the micellar media of SDS and CTABr, were performed by monitoring the absorbance at 426 nm. The reaction was started with the addition of calculated amount of adrenaline in the pre-equilibrated solution containing the fixed amounts of sodium hydroxide, surfactant and silver nitrate solutions. The increase in absorbance was measured until the reaction was completed to 3–4 half lives. The values of pseudo first order rate constant (k_ψ, s^{-1}) were calculated from the slopes of plots of ln (A_∞–A_t) versus time with the average values of linear regression coefficient, $r^2 \geq 0.98$. Each kinetic runs were repeated at least thrice. The observed values of rate constant were found to be reproducible within the error limits of ±5 %.

Results and discussion

Influence of [surfactants] on the rate of formation of silver nanoparticles (Ag-NPs)

Adrenaline undergoes autoxidation reactions with dissolved oxygen in the alkaline medium to form adrenochrome and other products. During the course of reaction between adrenaline and oxygen in the presence of NaOH, the absorbance values (with λ_{max} at 490 nm) initially increase with the progress of reaction. The absorbance values reach to maxima, and thereafter, decrease rapidly in the visible region, whereas, the absorbance in the uv-region (with λ_{max} at 290 nm) continues to increase progressively with the formation of adrenochrome [34]. However, the addition of silver nitrate solution to the solution containing adrenaline and NaOH gave deep orange color solution having λ_{max} at 426 nm. The strong absorbance in the vicinity of 426 nm is attributed to the formation of Ag-nano particles (Ag-NPs). The nano sized crystallites of silver atoms appear colored due to the excitation of surface plasmons of colloidal silver sols formed through the reduction of silver ions by adrenaline. The broad band of absorption observed in the UV–visible spectrum for metallic nanoparticles is due to surface plasmon band (SPB) [35–37]. Silver atoms or ions do not absorb any radiations in the visible range, but, after their agglomerations into nanoparticles, they become orange colored owing to the excitation of the surface plasmons of nanoparticles formed. The SPB has strong absorption for nanoparticles with sizes greater than 2 nm. The position, shape and the intensity of the SPB strongly depends upon (1) dielectric constant of the surrounding medium (2) the electronic interactions between the stabilizing ligands and the nanoparticle, and (3) the size, shape and monodispersity of the nanoparticles. Thus, the strong absorption by the solution is due to the contribution of micellar environment, the interaction between the Ag-NPs and surrounding environment, and, the size and the size-distribution of the Ag-NPs. The SDS and CTABr micelles stabilized the Ag-NPs in the aqueous solution and prevented further agglomeration to form precipitate.

The repetitive scans were recorded for the formation of silver nanoparticles in the micellar medium containing fixed [SDS] (=5.0×10^{-3} mol dm^{-3}), [$AgNO_3$] (=2.0×10^{-4} mol dm^{-3}), [NaOH] (=1.0×10^{-3} mol dm^{-3}) and [adrenaline] (=2.0×10^{-5} mol dm^{-3}) taken into 3 mL cuvette at 25.0 ± 0.1 °C and are shown in Fig. 1. These spectra were recorded at the intervals of 2 min. The analysis of spectra presented in Fig. 1 reveal that the values of absorbance increase as the reaction proceeds and the maximum value of absorbance (λ_{max}) was observed at 426 nm. The influence of the variation in the concentrations of surfactants on the values of rate constant were studied in the concentration range from 2.0×10^{-3} mol dm^{-3} to 20.0×10^{-3} mol dm^{-3} SDS and 1.0×10^{-4} mol dm^{-3} to 12.5×10^{-4} mol dm^{-3} CTABr. The concentrations of $AgNO_3$ (=2.0×10^{-4} mol dm^{-3}), adrenaline (=2.0×10^{-5} mol dm^{-3}), and NaOH (=1.0×10^{-3} mol dm^{-3}) were kept constant at 25.0 ± 0.1 °C. The rate of agglomerations of silver atoms to form aggregated clusters was found to be dependent upon micelles concentrations. It is observed that the values of the rate

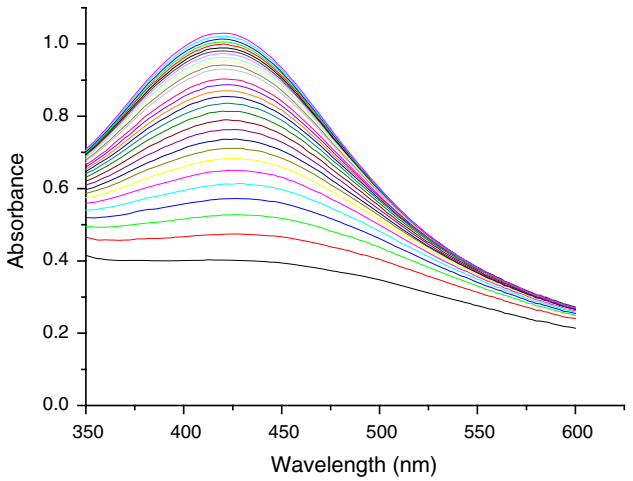

Fig. 1 Repetitive scan of the solution containing $[AgNO_3] = 2.0 \times 10^{-4}$ mol dm^{-3}, [adrenaline] $= 2.0 \times 10^{-5}$ mol dm^{-3}, [NaOH] $= 1.0 \times 10^{-3}$ mol dm^{-3} and [SDS] $= 5.0 \times 10^{-3}$ mol dm^{-3} at 25.0 ± 0.1 °C. The spectra were recorded at the interval of 2 min

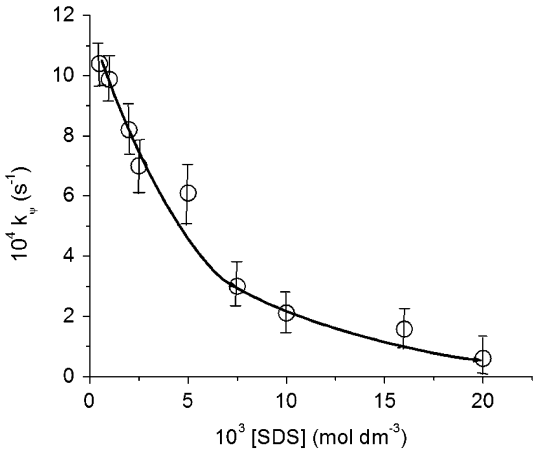

Fig. 2 Plot of k_ψ versus [SDS] at $[AgNO_3] = 2.0 \times 10^{-4}$ mol dm^{-3}, [adrenaline] $= 2.0 \times 10^{-5}$ mol dm^{-3} and [NaOH] $= 1.0 \times 10^{-3}$ mol dm^{-3} at 25.0 ± 0.1 °C

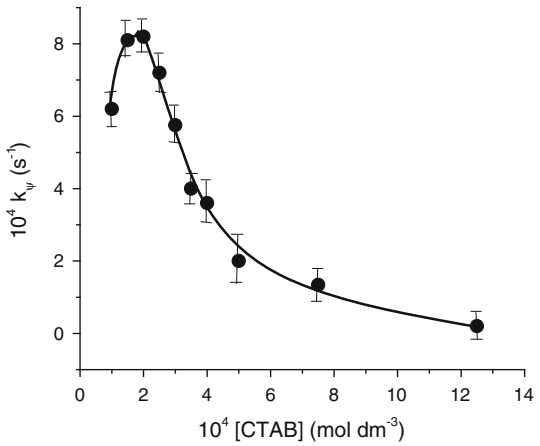

Fig. 3 Plot of k_ψ versus [CTABr] at $[AgNO_3] = 2.0 \times 10^{-4}$ mol dm^{-3}, [adrenaline] $= 2.0 \times 10^{-5}$ mol dm^{-3} and [NaOH] $= 1.0 \times 10^{-3}$ mol dm^{-3} at 25.0 ± 0.1 °C

constant decreases with the increase in [SDS] as displayed from the k_ψ-[SDS] profile (Fig. 2) while the values of rate constant increases initially with the increase in [CTABr], then reaches to a maximum value at 2.0×10^{-4} mol dm^{-3} CTABr. The further increase in the [CTABr] ([CTABr] $> 2.0 \times 10^{-4}$ mol dm^{-3}) decreases the rate of reaction (Fig. 3). The solution containing higher concentrations of CTABr or SDS ([SDS] $\geq 10.0 \times 10^{-3}$ mol dm^{-3} and [CTABr] $\geq 10.0 \times 10^{-4}$ mol dm^{-3}) did not yield orange colour and appeared almost colorless (Supplementary material S2, S3). The absence of orange colour in the presence of higher [surfactant] indicates that the reduced silver atoms could not aggregate together to form Ag-NPs. Thus, the agglomeration of silver atoms to form Ag-NPs occurs in the vicinity of lower concentrations of surfactants, i.e. [SDS] $\leq 10.0 \times 10^{-3}$ mol dm^{-3} and [CTABr] $\leq 10.0 \times 10^{-4}$ mol dm^{-3}.

The surfactant molecules in aqueous solution have tendency to form micelles which are dynamic aggregates of surfactant molecules having spherical, ellipsoidal, rod-like structures, depending upon the concentration of surfactant and ionic environment around it. Micelles of SDS and CTABr have their charged surfaces and non-polar core. They have highly anisotropic interfacial regions and possess the ability to alter the nanoparticle's shape, size and other surface properties; depending upon their nature of head group and length of hydrophobic tail. In dilute aqueous solutions, the molecules of SDS behave as strong electrolyte and dissociate into cationic Na^+ ion and anionic DS^- ions. The higher values of rate constant in the pre-micellar concentrations of SDS suggest the role of anionic headgroup and non-polar tail. The head part (DS^- anions) bind with the Ag^+ ions as counter ion while the tail part associates with adrenaline molecule. Thus, the DS^- anions bring the reactants; Ag^+ ions and adrenaline molecules in the close proximity, thereby, enhancing the rate of reduction of Ag^+ ions. The aggregation of the DS^- anions also causes the agglomeration of the Ag/Ag^+ to form nano-crystalline silver particles. The increase in [SDS] above its 'cmc' results into formation of micelles and the further increase in [SDS] cause the formation of more and more numbers of micelles. The micellization of SDS and increase in micelles concentrations (which relatively lower the concentration of Ag^+/Ag around the micellar surface) decrease the chance of agglomeration of Ag^+/Ag. Therefore, Ag^+/Ag fails to aggregate to form nano crystalline

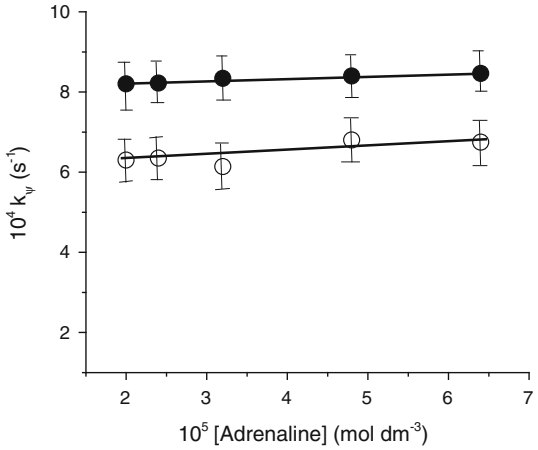

Fig. 4 Plot of k_ψ versus [adrenaline] at $[AgNO_3] = 2.0 \times 10^{-4}$ mol dm^{-3}, $[NaOH] = 1.0 \times 10^{-3}$ mol dm^{-3}, $[CTABr] = 2.0 \times 10^{-4}$ mol dm^{-3}(*filled circle*), $[SDS] = 5.0 \times 10^{-3}$ mol dm^{-3} (*open circle*) at 25.0 ± 0.1 °C

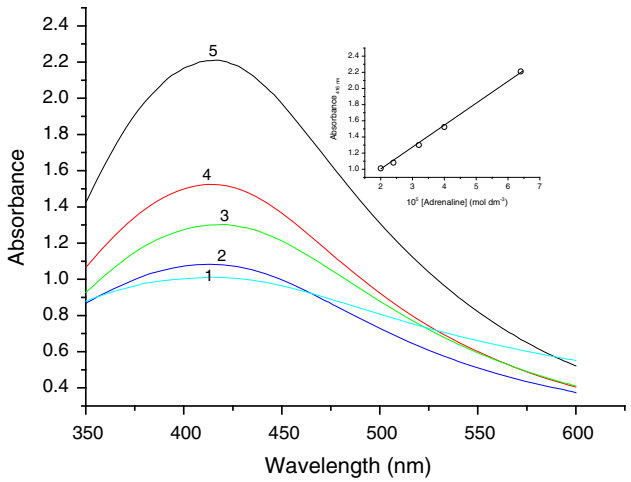

Fig. 5 Absorption spectra recorded at varying concentrations of adrenaline (2.0×10^{-5} mol dm^{-3} (1); 2.4×10^{-5} mol dm^{-3} (2); 3.2×10^{-5} mol dm^{-3} (3); 4.8×10^{-5} mol dm^{-3} (4); 6.4×10^{-5} mol dm^{-3} (5)). $[AgNO_3] = 2.0 \times 10^{-4}$ mol dm^{-3}, $[NaOH] = 1.0 \times 10^{-3}$ mol dm^{-3} and $[SDS] = 5.0 \times 10^{-3}$ mol dm^{-3} at 25.0 ± 0.1 °C. The inset plot is absorbance (at λ_{max}) versus [adrenaline]

silver particles at high [SDS] and, so, no orange colour appears. The observed variation (increase or decrease) in the values of rate constant with increase in [CTABr] may be explained in terms of the aggregation and dilution of the reactants concentrations in the micellar regions. The incorporations of adrenaline and silver ions in the Stern and palisade layers of CTABr micelles increases the local molalities of the reactants in the small volume and thereby increase the rate of reaction and also the rate of agglomeration of silver particles. However, the further increase in [CTABr] causes the dilution in reactants concentrations in the vicinity of micellar surface, so, the rate of reaction decreases. The silver ions/atoms associated with the different micelles fail to agglomerate to form Ag-NPs at higher concentrations of CTABr.

Influence of [adrenaline] on the rate of formation of silver nanoparticles (Ag-NPs)

The variation in the concentration of adrenaline on the rate of formation of Ag-NPs was studied in the range from 2.0×10^{-5} mol dm^{-3} to 6.4×10^{-5} mol dm^{-3} at 25 ± 0.1 °C. The concentrations of NaOH (=1.0×10^{-3} mol dm^{-3}), $AgNO_3$ (=2.0×10^{-4} mol dm^{-3}) and SDS (=5.0×10^{-3} mol dm^{-3})/CTABr (=2.0×10^{-4} mol dm^{-3}) were kept constant. Adrenaline reduces the Ag^+ ions into Ag-atom in the alkaline solution. The rate of reduction is quite fast, but, the rate of agglomeration of Ag-atoms to form Ag-NPs is slow. The values of rate constant were obtained after monitoring the increase in absorbance at different [adrenaline] as stated above. It is observed that the variation in [adrenaline] did not influence the values of rate constant as depicted in Fig. 4. The spectra presented in Fig. 5 show that absorbance increases with the increase in [adrenaline] and the straight line plot (in the inset figure) of absorbance at λ_{max} versus [adrenaline] suggest that the Beer-Lamber's laws have been obeyed for the formation of Ag-NPs at different concentration of adrenaline. The increase in [adrenaline] from 2.0×10^{-5} to 6.4×10^{-5} mol dm^{-3}, actually, increases the amount of reduced Ag atoms, thereby, increasing the number of Ag-NPs. Therefore, an increase in the values of absorbance is observed with the increase in [adrenaline] (Supplementary materials, S4).

Influence of [silver nitrate] on the rate of formation of silver nanoparticles (Ag-NPs)

The kinetic studies performed at different concentration of $AgNO_3$ demonstrate that the values of absorbance increase with increase in $[AgNO_3]$, and also, the colour yield depends linearly upon the $[AgNO_3]$ at fixed [adrenaline] and [NaOH]. The kinetic studies were performed at different initial concentrations of $AgNO_3$ in the range from 0.8×10^{-4} mol dm^{-3} to 2.4×10^{-4} mol dm^{-3} keeping [NaOH] (=1.0×10^{-3} mol dm^{-3}), [adrenaline] (=2.0×10^{-5} mol dm^{-3}) and [SDS] (=5.0×10^{-4} mol dm^{-3}) constant. The spectra are given in Fig. 6 and the inset figure shows the linear dependence of the maximum value of absorbance (λ_{max}) on $[AgNO_3]$. Thus, the Beer-Lambert's laws are followed at varying concentrations of $AgNO_3$. Figure 7 (k_ψ versus $[AgNO_3]$) shows that an increase in the $[AgNO_3]$ does not show any significant

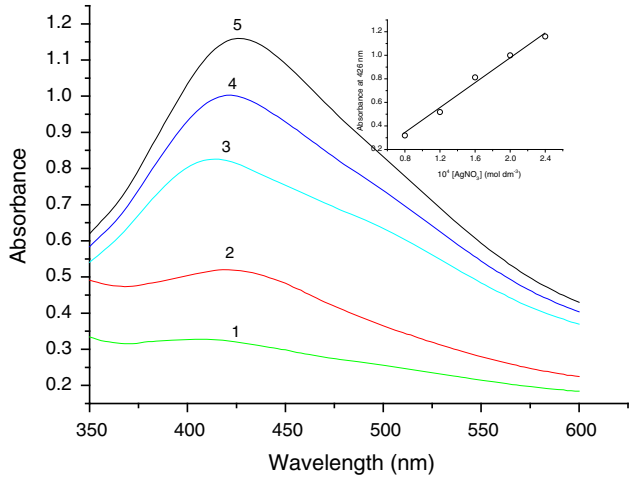

Fig. 6 Absorption spectra recorded at varying concentrations of silver nitrate [5.0×10^{-5} mol dm^{-3} (1); 1.2×10^{-4} mol dm^{-3} (2); 1.6×10^{-4} mol dm^{-3} (3); 2.0×10^{-4} mol dm^{-3} (4); 2.4×10^{-4} mol dm^{-3} (5)]. [Adrenaline] = 2.0×10^{-5} mol dm^{-3}, [NaOH] = 1.0×10^{-3} mol dm^{-3} and [SDS] = 5.0×10^{-3} mol dm^{-3} at 25.0 ± 0.1 °C. The inset plot is absorbance (at λ_{max}) versus [$AgNO_3$]

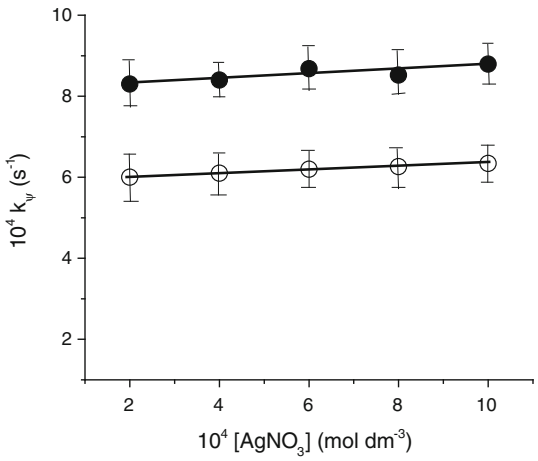

Fig. 7 Plot of k_ψ versus [$AgNO_3$] at [adrenaline] = 2.0×10^{-5} mol dm^{-3}, [NaOH] = 1.0×10^{-3} mol dm^{-3}, [CTABr] = 2.0×10^{-4} mol dm^{-3} (*filled circle*), [SDS] = 5.0×10^{-3} mol dm^{-3} (*open circle*) at 25.0 ± 0.1 °C

effect on the values of rate constant for the nanoparticles formation. The values of rate constant remain independent on [$AgNO_3$] in the presence of micelles of SDS as well as in the presence of CTABr. The increase in absorbance with the increase in [$AgNO_3$] is attributed to the increase in the amounts of nanoparticles formed. The independence of the values of rate constant on [$AgNO_3$] suggest that the reduction of Ag^+ ions are quite fast, but, the rate of agglomeration of silver atoms to form nanoparticles remains the same. The peak values of absorbance (λ_{max}) do not shift with the increase in [$AgNO_3$], thus, indicating that

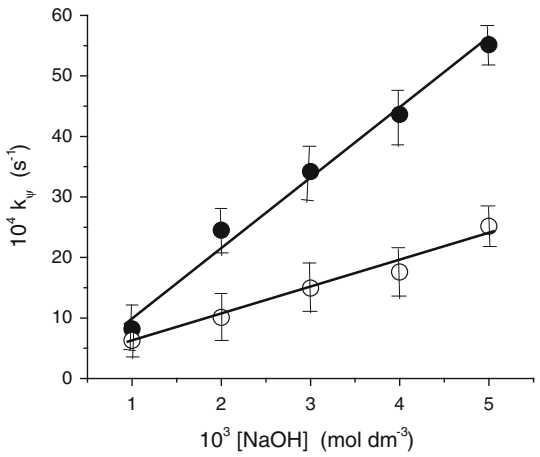

Fig. 8 Plot of k_ψ versus [NaOH] at [adrenaline] = 2.0×10^{-5} mol dm^{-3}, [$AgNO_3$] = 2.0×10^{-4} mol dm^{-3}, [CTABr] = 2.0×10^{-4} mol dm^{-3} (*filled circle*), [SDS] = 5.0×10^{-3} mol dm^{-3} (*open circle*) at 25.0 ± 0.1 °C

the particle size of Ag-NPs does not depend upon the [$AgNO_3$], rather it depends upon the reaction conditions (Supplementary material, S5).

Influence of [NaOH] on the rate of formation of silver nanoparticles (Ag-NPs)

The influence of different initial concentrations of NaOH on the rate of formation of Ag-NPs was studied in the range from 1.0×10^{-3} mol dm^{-3} to 5.0×10^{-3} mol dm^{-3}. The concentrations of adrenaline, $AgNO_3$, surfactant (CTABr/SDS) were kept constant at 2.0×10^{-5} mol dm^{-3}, 1.0×10^{-4} mol dm^{-3} and 2.0×10^{-4} mol dm^{-3}/5.0×10^{-4} mol dm^{-3}, respectively. The observed results are depicted graphically in Fig. 8, which shows that the rate constant values increase linearly with the increase in [NaOH]. The increase in [NaOH] increases the equilibrium concentration of silver oxide. The rate of oxidation of adrenaline by silver oxide (i.e. reduction of Ag^+ ions into Ag-atoms) also increases with the increase in [NaOH]. The hydroxide ions may also initiate the metal nucleation centres, which on further adsorption of silver metal atoms and metal ions lead to the formation of silver nanoparticles. Thus, the hydroxide ions activate the aggregation of silver oxide and silver atoms in the crystallization process and, thereby, increase the rate of reaction.

On the basis of the studies on the dependence in the values of rate constant on [adrenaline], [$AgNO_3$], [surfactant] and [NaOH], the following mechanism of the reaction in Scheme 1 is proposed. The rate of reduction of Ag^+ is fast accompanied with the formation of adrenochrome. But, after the reduction of Ag^+ ions, the aggregation of Ag atoms to form Ag-NPs is slow and dependent upon

Scheme1 Proposed mechanism of reduction of silver nitrate by adrenaline in the alkaline medium

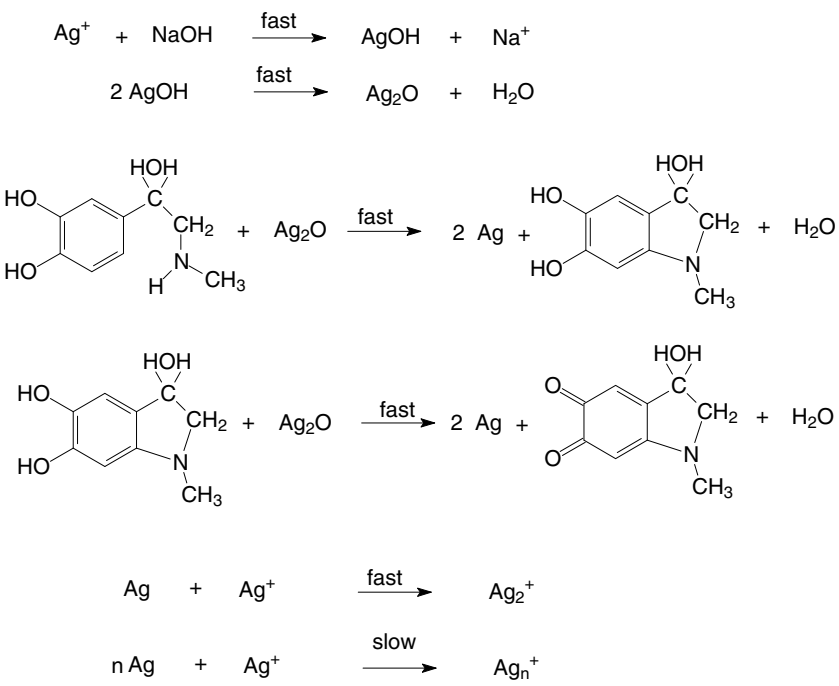

[surfactant] and [NaOH]. The aggregation of silver atoms to form nanoparticles is slow and is the rate determining step of the reaction. Therefore, with the increase in aggregation of Ag- atoms into Ag-NPs, the absorbance increases with time.

Analysis of TEM images and XRD spectra

Ag-NPs appear 'colored' owing to the oscillating conduction electrons. The TEM image presented in Fig. 9(b) reveals formation of predominantly spherical and some non spherical particles with their diameters between 30 and 60 nm. The existence of the polydispersity in the shapes and sizes of the nanoparticles may be attributed to the variation in the nucleation and growth rates of the nanoparticles. The median diameter of the nanoparticles formed was found to be approximately 43 nm [38, 39]. The electron diffraction studies carried out on a limited number of crystals indicate the presence of peaks at 2θ values of 37.42°, 43.64°, 63.98° and 77.05° which corresponds to (111), (200), (220) and (311) planes of silver crystals, respectively. Thus, the XRD spectrum given in Fig. 9(a) confirms the crystalline nature of silver nanoparticles having face-centered cubic crystal structure with lattice constant of 'a' ~4.076 Å in conformation with the reported value of 'a' = 4.086 Å (Joint Committee on Powder Diffraction Studies File No. 4-0783). The following relationships (1–5) were used to calculate the agglomeration number of Ag- atoms per nanoparticle:

$$\text{Edge length of each unit cell, '}a\text{'} = 4.076\ \text{Å} = 0.4076\ \text{nm} \quad (1)$$

$$\text{Volume of each unit cell} = 0.06732\text{nm}^3 \quad (2)$$

$$\text{Number of Ag} - \text{atoms per unit cell} = (1/8) \times \text{Number of atoms at corners} + (1/2) \times \text{Number of atoms at faces} = 4 \quad (3)$$

$$\text{Volume of spherical nanoparticle with diameter (43 nm)} = (4/3)\pi R^3 = 4.16 \times 10^4\ \text{nm}^3 \quad (4)$$

$$\text{Number of unit cells per nanoparticle} = (\text{Volume of nanoparticle})/(\text{volume of unit cell}) = 6.22 \times 10^5 \quad (5)$$

Therefore, the number of Ag- atoms per nanoparticle was found to be 2.49×10^6. In our experiment, we have taken 2×10^{-4} mol dm^{-3} $AgNO_3$ solution, i.e. 9.69×10^{13} nanoparticles per liter solution are formed. Assuming that, at the end of reaction all of the Ag^+ ions are reduced and crystallized in the form of nanoparticles with average values of diameter 43 nm, the number of moles of silver nanoparticles formed are 1.61×10^{-10} mol dm^{-3}. The extinction coefficient was calculated from the following relation (6).

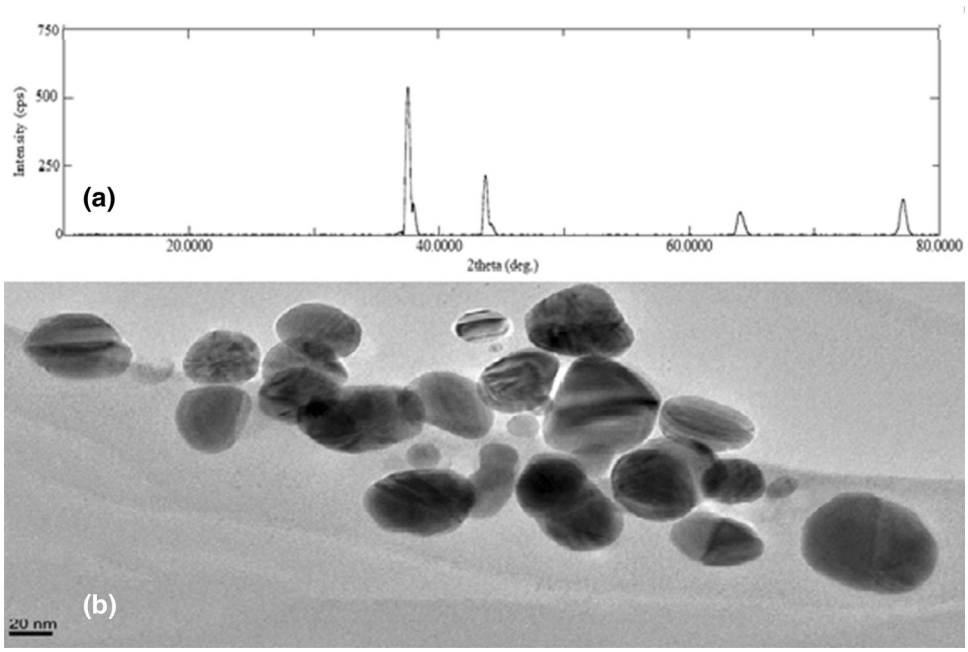

Fig. 9 **a** XRD patterns and **b** TEM image of silver nanoparticle crystals

$$A = \varepsilon b C \quad (6)$$

Where, 'A' is the absorbance, 'ε' is the molar extinction coefficient, '*b*' is path length (=1 cm) and 'C' is the molar concentration of nanoparticles. Thus, the obtained values of molar extinction coefficient (ε at $\lambda_{max} = 426$ nm) for the prepared nanoparticle is 6.34×10^9 mol^{-1} dm^3 cm^{-1}.

It is observed that the band width decrease with the increase in Ag^+ ions contents (Supplementary material, S1–S2). The bandwidth depends upon particle size due to the change in mean free path of the electrons and the decrease of the cluster size increases of the bandwidth. The broadening in the UV–Vis spectrum with the preserved maximum value of the absorption bands may be caused by the presence of silver particles with the same size but with different, spherical and nonspherical shapes [40].

Conclusion

The tendency of adrenaline to undergo autoxidation reaction in the alkaline media has been used as a potential reducing agent for the reduction of silver ions into silver nanoparticles. The Ag-NPs formed are almost spherical with face-centered cubic crystal structure. The size distribution of the Ag-NPs was found in the range 30–60 nm. The rate of reaction is quite fast and the values of rate constant were found to be independent of [adrenaline] and [$AgNO_3$]. The rate of reaction initially increased with increase in [CTABr], but, then decreased on further increasing the [CTABr]. The increase in [SDS] decreased the reaction rate. The addition of surfactant molecules prevented the settlement of the Ag-NPs. The increasing the concentration of sodium hydroxide increased the values of rate constant for the formation of Ag-NPs.

Acknowledgments The authors extend their appreciation to the Deanship of Scientific Research, College of Science Research Center, King Saud University, Riyadh, Saudi Arabia for supporting this project.

References

1. Yin Y, Li ZY, Zhong Z, Gates B, Xia Y, Venkateswaran S (2002) Synthesis and characterization of stable aqueous dispersions of silver nanoparticles through the tollens process. J Mater Chem 12:522–527
2. Cushing BL, Koleschineko VL, O'Connor CJ (2004) Recent advances in the liquid-phase syntheses of inorganic nanoparticles. Chem Rev 104:3893–3946
3. Burda C, Chen X, Narayanan R, El-Sayed MA (2005) The chemistry and properties of nanocrystals of different shapes. Chem Rev 105:1025–1102
4. Hosokawa M, Nogi K, Naito M, Yokoyam T (2008) Nanoparticle technology handbook. Jordan Hill, Oxford UK, pp 113–176
5. Rai M, Yadav A, Gade A (2009) Silver nanoparticles as a new generation of antimicrobials. Biotechnol Adv 27:76–83
6. García-Barrasa J, López-de-Luzuriaga JM, Monge M (2011) Silver nanoparticles: synthesis through chemical methods in solution and biomedical applications. Cent Eur J Chem 9:7–19
7. Abou El-Nour KMM, Eftaiha A, Al-Warthan A, Ammar RA (2010) Synthesis and applications of silver nanoparticles. Arab J Chem 3:135–140
8. Khomutov GB, Gubin SP (2002) Interfacial synthesis of noble metal nanoparticles. Mater Sci Eng, C 22:141–146
9. Oliveira MM, Ugarte D, Zanchet D, Zarbin AJG (2005) Influence of synthetic parameters on the size, structure, and stability of dodecanethiol-stabilized silver nanoparticles. J Colloid Interface Sci 292:429–435

10. Tsuji T, Iryo K, Watanabe N, Tsuji M (2002) Preparation of silver nanoparticles by laser ablation in solution: influence of laser wavelength on particle size. Appl Surf Sci 202:80–85
11. Pastoriza I, Liz-Marzan LM (2000) Reduction of silver nanoparticles in DMF. Formation of monolayers and stable colloids. Pure Appl Chem 72:83–90
12. Solomon SD, Bahadory M, Jeyarajasingam AV, Rutkowsky SA, Boritz C (2007) Synthesis of Silver Nanoparticles. J Chem Edu 84:322–325
13. Wong H II, Nersisyan H, Won CW, Lee JM, Hwang JS (2010) Preparation of porous silver particles using ammonium formate and its formation mechanism. J Chem Eng 156:459–464
14. Ong S, Wu J, Moochhala SM, Tan M, Lu J (2008) Development of a chitosan-based wound dressing with improved hemostatic and antimicrobial properties. Biomaterials 29:4323–4332
15. Li Y, Leung P, Yao L, Song QW, Newton E (2006) Antimicrobial effect of surgical masks coated with nanoparticles. J Hosp Infect 62:58–63
16. Mazeiko V, Kausaite-Minkstimiene A, Ramanaviciene A, Balevicius Z, Ramanavicius A (2013) Gold Nanoparticle and Conducting Polymer—Polyaniline—based Nanocomposites for Glucose Biosensor Design Sensors and Actuators B, 189: 187–193
17. Ramanaviciene A, Nastajute G, Snitka V, Kausaite A, German N, Barauskas-Memenas D, Ramanavicius A (2009) Spectrophotometric evaluation of gold nanoparticles as red-ox mediator for glucose oxidase. Sens Actuator B 137:483–489
18. Oztekin Y, Tok M, Bilici E, Mikoliunaite L, Yazicigil Z, Ramanaviciene A, Ramanavicius A (2012) Copper nanoparticle modified carbon electrode for determination of dopamine. Electrochim Acta 76:201–207
19. Yamamoto M, Nakamoto M (2003) Novel preparation of monodispersed silver nanoparticles via amineadducts derived from insoluble silver myristate in tertiary alkylamine. J Mat Chem 13:2064–2065
20. Kashiwagi Y, Yamamoto M, Nakamoto M (2006) Facile size-regulated synthesis of silver nanoparticles by controlled thermolysis of silver alkylcarboxylates in the presence of alkylamines with different chain lengths. J Colloid Interface Sci 300:169–175
21. Velikov KP, Zegers GE, van Blaaderen A (2003) Synthesis and characterization of large colloidal silver particles. Langmuir 19:1384–1389
22. Kurihara LK, Chow GM, Schoen PE (1995) Nanocrystalline metallic powders and films produced by the polyol method. Nanostruct Mater 5:607–613
23. Jacob JA, Kapoor S, Biswas N, Mukherjee T (2007) Size tunable synthesis of silver nanoparticles in water–ethylene glycol mixtures. Colloids Surf A Physicochem Eng Aspects 301:329–334
24. Raveendran P, Fu J, Wallen SL (2003) Completely "green" synthesis and stabilization of metal nanoparticles. J Am Chem Soc 125:13940–13941
25. Yu D, Yam VW-W (2004) Controlled synthesis of monodisperse silver nanocubes in water. J Am Chem Soc 126:13200–13201
26. Yu D, Yam VW-W (2005) Hydrothermal-induced as-sembly of colloidal silver spheres into various nano- particles on the basis of htab-modified silver mirror reaction. J Chem Phys B 109:5497–5503
27. Hussain S, Akrema Rahisuddin, Khan Zaheer (2014) Extracellular biosynthesis of silver nanoparticles: effects of shape-directing cetyltrimethylammonium bromide, pH, sunlight and additives. Bioprocess Biosyst Eng 37:953–964
28. Hussain S, Khan Zaheer (2014) Epigallocatechin-3-gallate-capped Ag nanoparticles: preparation and characterization. Bioprocess Biosyst Eng 37:1221–1231
29. Hussain S, Al-Thabaiti SA, Khan Zaheer (2014) Surfactant-assisted bio-conjugated synthesis of silver nanoparticles (Ag-NPs). Bioprocess Biosyst Eng 37:1727–1735
30. Bonevski R, Momirovic-Culjat J, Balint L (1978) Inhibition of epinephrine oxidation in weak alkaline solutions. J Pharm Sci 67:1474–1476
31. Grubstein B, Milano EA (1992) Stabilization of epinephrine in a local anesthetic injectable solution using reduced levels of sodium metabisulfite and edta. Drug Dev Ind Pharm 18:1549–1566
32. Broadley KJ, Penson PE (2004) The roles of alpha- and beta-adrenoceptor stimulation in myocardial ischaemia. Auton Autacoid Pharmacol 24:87–93
33. Al-Ayed AS, Al-Lohedan HA, Rafiquee MZA, Ali MS, Issa ZA (2013) Kinetics of the autoxidation of adrenaline and [copper(II)(adrenaline)]2+ in alkaline aqueous and micellar media. Transition Met Chem 38:173–181
34. Hoellein L, Holzgrabe U (2012) Ficts and facts of epinephrine and norepinephrine stability in injectable solutions. Int J Pharmac 434:468–480
35. Kelly KL, Coronado E, Zhao LL, Schatz GC (2003) The optical properties of metal nanoparticles: the influence of size, shape, and dielectric environment. J Phys Chem B 107:668–677
36. Hutter E, Fendler JH (2004) Exploitation of localized surface plasmon resonance. Adv Mater 16:1685–1706
37. Moores A, Goettmann F (2006) The plasmon band in noble metal nanoparticles: an introduction to theory and applications. New J Chem 30:1121–1132
38. Baia L, Simon S (2007) Modern research and educational topics in microscopy, A. Méndez-Vilas and J. Díaz (Eds.), ©FORMATEX 2007, pp 276–283
39. Baset S, Akbari H, Zeynali H, Shafie M (2011) Size measurement of metal and semiconductor nanoparticles via UV-vis absorption spectra. Dig J Nanomater Biostruct 6:709–716
40. Baia L, Baia M, Kiefer W, Popp J, Simon S (2006) Structural and morphological properties of silver nanoparticles—phosphate glass composites. Chem Phys 327:63–69